

# Flight Path Control of Unmanned Aerial Vehicle Considering Attitude-Hold

Hyeong-gwan Kang<sup>1</sup> and Youdan Kim<sup>1</sup>

<sup>1</sup> Aerospace Engineering, Seoul National University, Seoul, Republic of Korea

**Abstract.** A nonlinear flight path controller is designed for an unmanned aerial vehicle (UAV) to detect landmines. Due to the characteristics of the mine detection sensors, the allowable roll and pitch angle changes of the UAV are strictly limited. A sliding mode control scheme is used to design the flight path controller for the UAV considering the attitude-hold constraint. In addition, an extended high-gain observer is adopted to deal with wind disturbances. It is assumed that wind disturbance mainly affects the flight path control loop. The extended high-gain observer is applied to the flight path control loop to estimate the wind disturbances. The estimated disturbances are used in the sliding mode controller. Numerical simulations are performed to demonstrate the effectiveness of the proposed controller. Simulation results show that the proposed controller and the disturbance observer have a proper performance in flight path control of the UAV with the attitude-hold constraint and the existence of the wind disturbance.

**Keywords:** Sliding Mode Control (SMC), Extended High Gain Observer, Mine Detection.

## 1 Introduction

Clearing landmines in the battle field is a dangerous and time-consuming operation. Recent studies show that unmanned aerial vehicles (UAVs) may be useful for the detection of the explosives over a wide area. However, due to the characteristics of the mine detection sensors, the allowable roll and pitch angle changes of the UAV are strictly limited, even under the existence of a wind disturbance. Therefore, a robust flight path controller for the UAV considering the attitude-hold constraint should be designed.

Several researches have been done for the control design considering the attitude-hold constraint. A pitch hold controller for a fighter jet was designed using fuzzy logic [1]. Terrain-following controller of an UAV with the pitch-hold constraint was designed [2]. However, only the pitch-hold was considered and the wind disturbance was not considered in these researches.

Various robust control techniques including sliding mode control have been developed. A flight path control of F/A-18 model with the model uncertainty was designed using an adaptive sliding mode control scheme [3]. Fault tolerant adaptive

sliding mode controller was designed for a fixed-wing UAV [4]. Position tracking controller was designed for a quadrotor UAV under the model uncertainty and wind disturbance using a sliding mode control [5-6]. To deal with a disturbance more efficiently, a disturbance observer can be combined with the robust controller. A high-gain observer was used to estimate an unknown disturbance and combined with a sliding mode controller [7].

In this study, a sliding mode flight path controller is designed considering the attitude-hold constraint. An extended high-gain observer is utilized to estimate the wind disturbance. The estimated wind disturbance is used in the sliding mode controller improve the robustness of the designed controller. The performance of the proposed algorithms is demonstrated through a numerical simulation.

## 2 Sliding Mode Control Design

The control objective in this study is to steer the true airspeed, flight path angle, and course angle to track their reference signals while maintaining the pitch and the roll angle to their trim values. To achieve the control objective, a controller which controls the true airspeed, flight path angle, course angle, roll angle, and the pitch angle should be designed. In this study, the sliding mode controller which achieves the control objective by using the thrust, lift and moment as a control input is proposed. The sliding mode controller proposed in this study consists of three loops: flight path control loop, attitude control loop, and body angular rate control loop as shown in Fig. 1. In each loop, the sliding mode control is designed to achieve the control objective of the control loop.

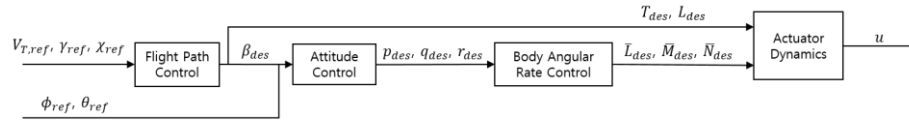


Fig. 1. Control loop structure for sliding mode control design

### 2.1 Flight Path Control Loop

In the flight path control loop, the true airspeed  $V_T$ , the flight path angle  $\gamma$ , and the course angle  $\chi$  are controlled to follow their reference signals. The available (virtual) controls in this loop are the thrust  $T$ , the lift  $L$  and the sideslip angle  $\beta$ . The equations of motion of this control loop are represented as

$$\dot{x}_1 = \begin{bmatrix} \frac{1}{m} (-D + T \cos \alpha \cos \beta) - g \sin \gamma \\ \frac{1}{mV_T} (L \cos \mu - Y \sin \mu + T(\sin \alpha \cos \mu + \cos \alpha \sin \beta \sin \mu)) - \frac{g}{V_T} \cos \gamma \\ \frac{1}{mV_T \cos \gamma} (L \sin \mu + Y \cos \mu + T(\sin \alpha \sin \mu - \cos \alpha \sin \beta \cos \mu)) \end{bmatrix} \quad (1)$$

where  $x_1 = [V_T \ \gamma \ \chi]^T$ ,  $m$  is the mass of the UAV,  $\mu$  is the aerodynamic roll angle,  $\alpha$  is the angle of attack,  $g$  is the gravitational constant,  $Y$  is the side force and  $D$  is the drag. Note that the control variables  $T$  and  $\beta$  are not affine in the equations of motion. Therefore, a new control variable  $v$  for the flight path control loop is defined as

$$v = \begin{bmatrix} v_1 \\ v_2 \\ v_3 \end{bmatrix} = \begin{bmatrix} T \cos \alpha \cos \beta \\ T(\sin \alpha \cos \mu + \cos \alpha \sin \beta \sin \mu) + L \cos \mu - Y \sin \mu \\ T(\sin \alpha \sin \mu - \cos \alpha \sin \beta \cos \mu) + L \sin \mu + Y \cos \mu \end{bmatrix} \quad (2)$$

The equations of motion can be modified using  $v$  as

$$\dot{x}_1 = f_1 + G_1 v = \begin{bmatrix} -\frac{D}{m} - g \sin \gamma \\ -\frac{g \cos \gamma}{V_T} \\ 0 \end{bmatrix} + \begin{bmatrix} \frac{1}{m} & 0 & 0 \\ 0 & \frac{1}{mV_T} & 0 \\ 0 & 0 & \frac{1}{mV_T \cos \gamma} \end{bmatrix} v \quad (3)$$

The control objective is to make  $x_1$  follow the reference signals  $x_{1,ref} = [V_{T,ref} \ \gamma_{ref} \ \chi_{ref}]^T$ , and therefore the sliding variable  $s_1$  for the flight path control loop is defined as

$$s_1 = x_1 - x_{1,ref} \quad (4)$$

Let us consider the following Lyapunov function.

$$V_1 = \frac{1}{2} s_1^T s_1 \quad (5)$$

The derivative of  $V_1$  is given by

$$\dot{V}_1 = s_1^T (f_1 + G_1 v - \dot{x}_{1,ref}) \quad (6)$$

From(6), the control law for making  $\dot{V}_1$  negative can be chosen as

$$v_{des} = G_1^{-1}(-f_1 + \dot{x}_{1,ref} - K_1 \text{sgn}(s_1))$$

where  $K_1 > 0$  is a control gain matrix. Now, let us determine the desired control values  $T_{des}$ ,  $L_{des}$ , and  $\beta_{des}$ . From (2), the following equations can be derived.

$$T_{des} = \frac{v_1}{\cos \alpha \cos \beta} \quad (7)$$

$$L_{des} = v_2 \cos \mu + v_3 \sin \mu - T_{des} \sin \alpha \quad (8)$$

$$Y_{des} = -v_2 \sin \mu + v_3 \cos \mu + T_{des} \cos \alpha \sin \beta \quad (9)$$

It is assumed that the desired side force  $Y$  can be decomposed as

$$Y_{des} = Y_0 + Y_\beta \beta_{des} \quad (10)$$

where  $Y_0$  is the side force component which is independent to  $\beta$ . The desired sideslip angle  $\beta_{des}$  is obtained using (10) as

$$\beta_{des} = \frac{Y_{des} - Y_0}{Y_\beta} \quad (11)$$

The desired thrust  $T_{des}$  and the lift  $L_{des}$  calculated in this control loop are directly used as a control input. On the other hand, the desired sideslip angle  $\beta_{des}$  is used as a reference signal for the attitude control loop to find the desired angular rate value.

## 2.2 Attitude Control Loop

Controller for the attitude control loop makes the sideslip angle  $\beta$  track its desired value  $\beta_{des}$ , and the roll angle  $\phi$  and the pitch angle  $\theta$  track their reference signals. The angular rate for each body axis  $p$ ,  $q$ , and  $r$  are used as the virtual controls in this loop. The equations of motion of this loop can be described as

$$\dot{x}_2 = f_2 + G_2 x_3 = \begin{bmatrix} \frac{Y-T \cos \alpha \sin \beta}{mV_T} + \frac{g \sin \mu \cos \gamma}{V_T} \\ 0 \\ 0 \end{bmatrix} + \begin{bmatrix} \sin \alpha & 0 & -\cos \alpha \\ 1 & \tan \theta \sin \phi & \tan \theta \cos \phi \\ 0 & \cos \phi & -\sin \phi \end{bmatrix} x_3 \quad (12)$$

where  $x_2 = [\beta \ \phi \ \theta]^T$ , and  $x_3 = [p \ q \ r]^T$ .

Considering the control objective of this step, the sliding variable  $s_2$  for the attitude control loop is chosen as

$$s_2 = x_2 - x_{2,ref} \quad (13)$$

where  $x_{2,ref} = [\beta_{des} \ \phi_{ref} \ \theta_{ref}]^T$ , and  $\phi_{ref}$  and  $\theta_{ref}$  are the reference signals of  $\phi$  and  $\theta$ , respectively. Now, consider the following Lyapunov function for this loop.

$$V_2 = \frac{1}{2} s_2^T s_2 \quad (14)$$

The derivative of  $V_2$  is obtained as

$$\dot{V}_2 = s_2^T (f_2 + G_2 x_3 - \dot{x}_{2,ref}) \quad (15)$$

To make  $\dot{V}_2$  negative, the control law can be chosen as

$$x_{3,des} = \begin{bmatrix} p_{des} \\ q_{des} \\ r_{des} \end{bmatrix} = G_2^{-1} \left( -f_2 + \begin{bmatrix} 0 \\ \dot{\phi}_{ref} \\ \dot{\theta}_{ref} \end{bmatrix} - K_2 \text{sgn}(s_2) \right) \quad (16)$$

where  $K_2 > 0$  is a gain matrix. Note that the derivative of  $\beta_{des}$  is difficult to be analytically calculated, and therefore it is considered as an uncertainty in this study.

### 2.3 Body Angular Rate Control Loop

In the body angular rate control loop, the control objective is to steer the body angular rate of each axis  $p$ ,  $q$ ,  $r$  to follow the desired values which are obtained from the attitude control loop. In this loop, the available controls are the moment of each body axis  $\bar{L}$ ,  $\bar{M}$ , and  $\bar{N}$ . The equations of motion can be described as

$$\dot{x}_3 = f_3 + G_3 u_m = \begin{bmatrix} (c_1 r + c_2 p)q \\ c_5 p r - c_6 (p^2 - r^2) \\ (c_8 p - c_2 r)q \end{bmatrix} + \begin{bmatrix} c_3 & 0 & c_4 \\ 0 & c_7 & 0 \\ c_4 & 0 & c_9 \end{bmatrix} u_m \quad (17)$$

where  $u_m = [\bar{L} \ \bar{M} \ \bar{N}]^T$ , and the definition of the inertia terms  $c_i$  ( $i = 1, \dots, 9$ ) are given in Appendix [8].

The sliding variable  $s_3$  and the Lyapunov function  $V_3$  of this loop are chosen as

$$s_3 = x_3 - x_{3,des} \quad (18)$$

$$V_3 = \frac{1}{2} s_3^T s_3 \quad (19)$$

The derivative of  $\dot{V}_3$  is obtained as

$$\dot{V}_3 = s_3^T (f_3 + G_3 u_m - \dot{x}_{3,des}) \quad (20)$$

To make  $\dot{V}_3$  negative, the control law is chosen as

$$u_m = G_3^{-1} (-f_3 - K_3 \text{sgn}(s_3)) \quad (21)$$

where  $K_3 > 0$  is a control gain matrix. Note that  $\dot{x}_{3,des}$  is considered as an uncertainty because it is difficult to obtain  $\dot{x}_{3,des}$  analytically. Finally, moment command  $u_m$  is combined with the thrust command and the lift commands which are obtained in the flight path control loop, to be used as a control input.

### 2.4 Control Input Dynamics

The desired value of the thrust, lift, and moment obtained from the previous subsections are used as a control input command. The dynamics for this control input is modeled as a first-order system with the transfer function of

$$G_c(s) = \frac{1}{\tau s + 1} \quad (22)$$

where  $\tau$  is a time constant.

## 3 Wind Disturbance Observer Design

In this study, it is assumed that the wind disturbance mainly affects the equations of motion in the flight path control loop. Therefore, the wind disturbance observer is designed to estimate the wind disturbance in the flight path control loop. Considering

the wind disturbance, the equations of motion of the flight path control loop are represented by

$$\dot{x}_1 = f_1 + G_1 v + d \quad (23)$$

Assume that  $\dot{d}$  is bounded. The extended high-gain observer is designed as follows,

$$\dot{\hat{x}}_1 = f_1 + G_1 v + \hat{d} + a_1 \frac{x_1 - \hat{x}_1}{\epsilon} \quad (24)$$

$$\dot{\hat{d}} = a_2 \frac{x_1 - \hat{x}_1}{\epsilon^2} \quad (25)$$

where  $0 < \epsilon \ll 1$  is the time constant,  $\hat{x}_1$  and  $\hat{d}$  are the estimates of  $x_1$  and  $d$ , respectively, and  $a_1$  and  $a_2$  are the positive constants which are selected to make the polynomial  $x^2 + a_1 x + a_2$  Hurwitz. Using  $\hat{d}$ , the control law of the flight path control loop is modified as

$$v_{des} = (-f_1 - \hat{d} + \dot{x}_{1,ref} - K_1 \text{sgn}(s_1)) \quad (26)$$

To check the stability of the proposed observer, let us define the error variables  $e_{x_1}$  and  $e_d$  as

$$e_{x_1} = \frac{x_1 - \hat{x}_1}{\epsilon} \quad (27)$$

$$e_d = d - \hat{d} \quad (28)$$

Then, we have

$$\epsilon \begin{bmatrix} \dot{e}_{x_1} \\ \dot{e}_d \end{bmatrix} = \begin{bmatrix} -a_1 I_3 & I_3 \\ -a_2 I_3 & 0 \end{bmatrix} \begin{bmatrix} e_{x_1} \\ e_d \end{bmatrix} + \epsilon \begin{bmatrix} 0 \\ I_3 \end{bmatrix} \dot{d} \quad (29)$$

where  $I_3$  is a  $3 \times 3$  identity matrix. Assuming that  $\dot{d}$  is bounded,  $e_{x_1}$  and  $e_d$  are exponentially stable [9].

## 4 Numerical Simulations

### 4.1 Simulation Settings

Numerical simulation is performed to demonstrate the effectiveness of the proposed controller. The ARGOS-I UAV model is used in the simulation. The initial flight condition of the UAV is set as the trim condition with the speed of 25 m/s, and zero flight path angle. During the simulation, the reference signals of the true airspeed, the flight path angles and the course angle are set as the trim speed 25 m/s,  $2^\circ$ , and  $t/16$  rad, respectively, where  $t$  is the simulation time expressed in seconds. Also, the reference signals of the pitch and the roll angle are given as the trim values. The speed of the external wind is expressed as 5 m/s in  $x$  and  $y$  axis in the inertial frame, respectively. The control gains, and coefficients for the controller and the disturbance observer are summarized in Table 1.

**Table 1.** Control gains and other coefficients

Parameter	Value
$K_1$	diag(1,1,5)
$K_2$	diag(1,1,1)
$K_3$	diag(10,10,10)
$\tau$	0.1
$\epsilon$	0.1
$a_1$	$3I_3$
$a_2$	$I_3$

#### 4.2 Simulation Results

Fig. 2 shows the time response of the true airspeed, flight path angle, course angle, roll angle, pitch angle and their command, with or without the wind disturbance observer. It is observed that the proposed sliding mode controller has a good performance on the roll and the pitch angle tracking, even without using the disturbance observer. However, there exist steady-state errors in tracking the true airspeed and the flight path angle when the disturbance observer is not used. It is also observed that the steady-state errors in the true airspeed and the flight path angle tracking are reduced when the disturbance observer is used, while the tracking performance on the roll and the pitch angle is not degraded. The root-mean-squared error (RMSE) values of the variables after 4 seconds are summarized in Table 2. The RMSE values of the variables except the flight path angle is lower when the disturbance observer is used.

**Table 2.** Tracking performance

	RMSE	
	w/o DoB	w/ DoB
$V_T$	0.1163 m/s	0.0060 m/s
$\gamma$	0.1739°	0.0913°
$\chi$	1.3379°	1.8349°
$\phi$	0.00000418°	0.00000350°
$\theta$	0.000305°	0.000195°

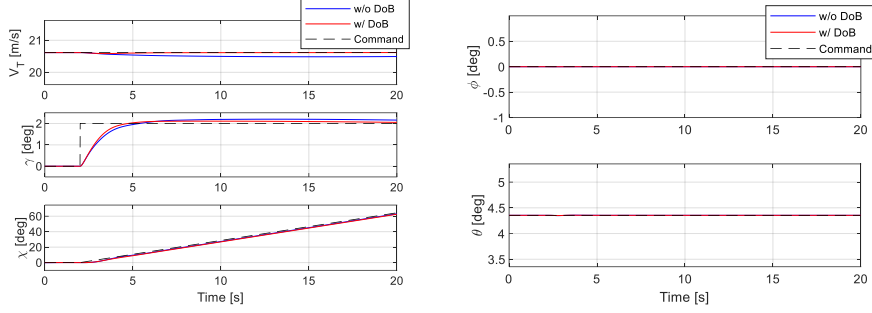


**Fig. 2.** Time response of  $V_T$ ,  $\gamma$ ,  $\chi$ ,  $\phi$  and  $\theta$

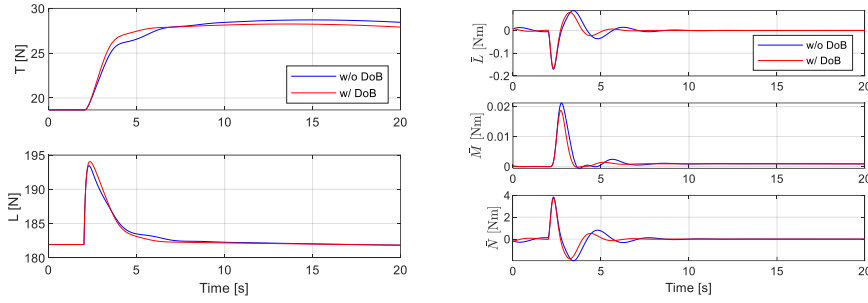


**Fig. 3.** Time response of thrust, lift and moment

## 5 Conclusion

Nonlinear flight path controller was designed for an unmanned aerial vehicle by using the sliding mode control scheme. In control design, the control loop structure was proposed considering the attitude-hold constraint. Wind disturbance observer was also designed based on the extended high-gain observer to deal with the unknown wind disturbance. Numerical simulation was carried out to demonstrate the effectiveness of the proposed control scheme.

## Appendix

$$\begin{aligned}
 c_1 &= \frac{(J_y - J_z)J_z - J_{xz}^2}{J_x J_z - J_{xz}^2}, \quad c_2 = \frac{(J_x - J_y + J_z)J_{xz}}{J_x J_z - J_{xz}^2}, \quad c_3 = \frac{J_z}{J_x J_z - J_{xz}^2} \\
 c_4 &= \frac{J_{xz}}{J_x J_z - J_{xz}^2}, \quad c_5 = \frac{J_z - J_x}{J_y}, \quad c_6 = \frac{J_{xz}}{J_y} \\
 c_7 &= \frac{1}{J_y}, \quad c_8 = \frac{J_x(J_x - J_y) + J_{xz}^2}{J_x J_z - J_{xz}^2}, \quad c_9 = \frac{J_x}{J_x J_z - J_{xz}^2}
 \end{aligned} \tag{30}$$



## Acknowledgement

This research has been supported by the Defense Challengeable Future Technology Program of the Agency for Defense Development, Republic of Korea.

## References

1. Bossert, D., Cohen, K.: Design of Fuzzy Pitch Attitude Hold Systems for a Fighter Jet. AIAA Guidance, Navigation, and Control Conference and Exhibit, Montreal, Canada (2001).
2. Kang, H., Lee, S., Lee, J., Kim, Y., Suk, J., Kim, S.: Altitude Tracking of UAV with Pitch-Hold Constraint Based on Model Predictive Control for Mine Detection, 2021 21<sup>st</sup> International Conference on Control, Automation and Systems, Jeju, Korea (2021).
3. Singh, S., Steinberg, M., Page, A.: Nonlinear Adaptive and Sliding Mode Flight Path Control of F/A-18 Model. *IEEE Transactions of Aerospace and Electronic Systems* 39(4), 1250-1262 (2003).
4. Ahn, C., Kim, Y., Kim, H.: Adaptive Sliding Mode Controller Design for Fault Tolerant Flight Control Systems. AIAA Guidance, Navigation, and Control Conference, Key Stone, Co (2006).
5. Perozzi, G., Efimov, D., Biannic, J., Planckaert, L., Coton, P.: On Sliding Mode Control Design for UAV Using Realistic Aerodynamic Coefficients. *IEEE 56<sup>th</sup> Annual Conference on Decision and Control*, Melbourne, Australia (2017).
6. Mofid, O., Mobayen, S., Zhang, C., Esakki, B.: Desired Tracking of Delayed Quadrotor UAV Under Model Uncertainty and Wind Disturbance Using Adaptive Super-Twisting Terminal Sliding Model Control. *ISA Transactions* 123, 455-471 (2022).
7. Oh, S., Khalil, H.: Nonlinear Output-Feedback Tracking Using High-Gain Observer and Variable Structure Control. *Automatica* 33(10), 1845-1856 (1997).
8. Stevens, B., Lewis, F.: *Aircraft Control and Simulation*. Wiley, New York, NY (1992).
9. Khalil, H.: High-Gain Observers in Nonlinear Feedback Control. *International Conference on Control, Automation and Systems*, Seoul, Korea (2008).